X-ray Irradiation Induced Reversible Resistance Change in Pt/TiO_2/Pt Cells

Seo Hyoung Chang,[†] Jungho Kim,[‡,*] Charudatta Phatak,[§] Kenneth D'Aquila,[†,§,⊥] Seong Keun Kim,[∥,#] Jiyoon Kim,[†,▽] Seul Ji Song,[#] Cheol Seong Hwang,[#] Jeffrey A. Eastman,[†] John W. Freeland,[‡] and Seungbum Hong[†,§,▽,*]

[†]Materials Science Division, Argonne National Laboratory, Lemont, Illinois 60439, United States, [‡]Advanced Photon Source, Argonne National Laboratory, Lemont, Illinois 60439, United States, [§]Nanoscience and Technology Division, Argonne National Laboratory, Lemont, Illinois 60439, United States, [⊥]Department of Materials Science and Engineering, Northwestern University, Evanston, Illinois 60208, United States, [∥]Korea Institute of Science and Technology, Seoul 136-791, Korea, [#]WCU Hybrid Materials Program, Department of Materials Science and Engineering and Inter-university Semiconductor Research Center, Seoul National University, Seoul 151-744, Korea, and [▽]Department of Materials Science and Engineering, KAIST, Daejeon 305-701, Korea

ABSTRACT The interaction between X-rays and matter is an intriguing topic for both fundamental science and possible applications. In particular, synchrotron-based brilliant X-ray beams have been used as a powerful diagnostic tool to unveil nanoscale phenomena in functional materials. However, it has not been widely investigated how functional materials respond to the brilliant X-rays. Here, we report the X-ray-induced reversible resistance change in 40-nm-thick TiO_2 films sandwiched by Pt top and bottom electrodes, and propose the physical mechanism behind the emergent phenomenon. Our findings indicate that there exists a photovoltaic-like effect, which modulates the resistance reversibly by a few orders of magnitude, depending on the intensity of impinging X-rays. We found that this effect, combined with the X-ray irradiation induced phase transition confirmed by transmission electron microscopy, triggers a nonvolatile reversible resistance change. Understanding X-ray-controlled reversible resistance changes can provide possibilities to control initial resistance states of functional materials, which could be useful for future information and energy storage devices.

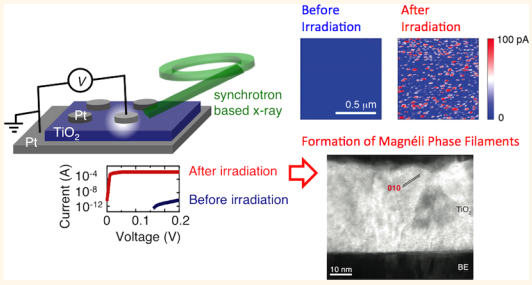

KEYWORDS: resistive switching · X-ray irradiation · photovoltaic effect · Magnéli phase · Joule heating · defect generation

The interaction between X-rays and matter has attracted much attention from academia, national laboratories and industries.[1,2] Synchrotron-based X-ray radiation has been widely used to probe microscopic phenomena and to characterize functional materials properties.[3,4] For instance, researchers used X-ray absorption near edge spectroscopy to elucidate the oxygen vacancy induced resistance change at the nanoscale by probing the valence of Cr atoms in Cr-doped $SrTiO_3$ and reduced TiO_2 phases for resistive switching memory devices.[5,6]

X-ray irradiation can alter the charge and orbital states of strongly correlated systems[7−9] and perturb the bonds of soft materials.[10] As such, radiation-induced change in chemistry has been the subject of great interest for long time and a large literature shows that TiO_2 plays the role of a reference material for the loss of oxygen *via* photon-stimulated desorption involving an interatomic Auger process, which leads to an irreversible resistance change.[11,12]

Resistive switching phenomena in metal−insulator−metal (MIM) structures have been investigated intensively for future nanoscale nonvolatile memory devices,[13,14] nanoionic switches,[15] and adaptive electronic components like the human brain.[16] One of the well-studied materials is TiO_2, which exhibits bistable or multiple resistance states induced *via* movement of oxygen defects by external electrical stimuli.[13,17] TiO_2 shows either bipolar or unipolar resistive switching. In the case of unipolar switching, only one bias polarity is needed for both set (on) and reset (off) processes.[18,19] Unipolar resistive switching originates from the formation and rupture of nanoscale conducting paths under electric stimuli.[20−22] Because the change of resistance state is sensitive to the perturbation of conducting paths in thin films,[18−22] we envision that resistive switching materials can serve as an ideal system to monitor

* Address correspondence to hong@anl.gov, jhkim@aps.anl.gov.

Received for review November 12, 2013 and accepted January 13, 2014.

Published online January 13, 2014
10.1021/nn405867p

the interaction between an X-ray beam and the reversible formation and rupture of conduction paths in nanoscale structures.

Here, we describe the results of an investigation of the interaction between TiO_2 thin films and synchrotron-based X-rays, focusing on X-ray irradiation-induced volatile and nonvolatile reversible resistance changes rather than the irreversible resistance change induced by, for example, the Knotek–Feibelman mechanism[12] in Pt/TiO_2/Pt memory cells, which could be related to the formation of conduction channels within the oxide film. We found that a volatile reversible change results from a photovoltaic-like effect, and we discuss the origins of the resistance change. In addition, we examined how X-ray irradiation affects the nonvolatile reversible resistance change using conducting atomic force microscopy (C-AFM) and transmission electron microscopy (TEM).

RESULTS

Resistive Switching Characteristics. First, we investigated the unipolar resistive switching characteristics of our Pt/TiO_2/Pt cells. As shown in Figure 1a, a cell exhibited a typical unipolar memory resistive switching behavior, which is in accordance with a previous report.[18] Initially, the resistance of the pristine cell was high and showed an insulating state. When we increased the bias voltage above 4 V, the resistance changed by an electroforming process to a low resistance state (LRS) (see Figure 1a). When we applied about 0.55 V, the LRS reset into a high resistance state (HRS). By controlling the bias voltage, HRS (LRS) changed into LRS (HRS) in a reversible manner.

X-ray Irradiation Effect. We exposed a pristine sample to the synchrotron X-ray beam with incident energy set at 8.3 keV, which is larger than Ti K-absorption edge (4.97 keV), and high photon flux (2×10^7 photons/(μm^2 s)). We observed significant resistance changes of the pristine state of our Pt/TiO_2/Pt cells induced by the X-ray irradiation. Figure 1b illustrates a schematic of the sample configuration for the electrical measurements made under X-ray irradiation at Sector 9ID, Advanced Photon Source at Argonne National Laboratory. The typical pristine state shows highly insulating behavior with a current level of 10^{-12} to 10^{-9} A at 0.2 V, as shown in Figure 1b. To our surprise, after 24 h exposure to the X-ray beam, the cell changed into LRS and the current flow at 0.2 V was limited by the compliance current, 0.01 A (see lower panel current – voltage curves in Figure 1b). We tested five more Pt/TiO_2/Pt cells to check the reproducibility of the phenomenon and confirmed the uniform resistance change of our cells.

As seen in Figure 2, we monitored the time-dependent resistance changes, by measuring the current level at 0.2 V every second. We found that there were two processes responsible for the resistance change induced

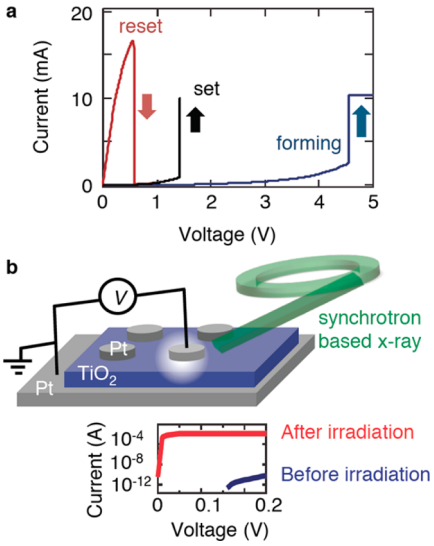

Figure 1. Resistive switching phenomenon. (a) A Pt/TiO_2/Pt cell shows typical current–voltage (I–V) characteristics of unipolar resistance switching (RS): the pristine state before forming, low resistance state (LRS) after set, and high resistance state (HRS) after reset. (b) Schematic of electrical measurement of a Pt/TiO_2/Pt cell with the synchrotron-based X-ray irradiation. The I–V curves of the cell, measured before and after the prolonged irradiation.

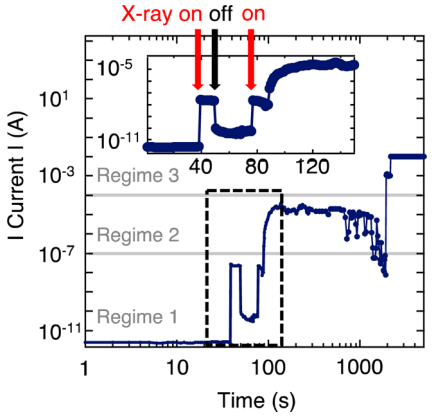

Figure 2. Time-dependent X-ray-irradiation effect. The current level of a Pt/TiO_2/Pt cell at 0.2 V was changed. The compliance current level of the cell was 0.01 A. The inset enlarged the dashed area. The shutter of X-ray beam opened at 39 s and opened again at 77 s.

by the X-ray irradiation: volatile and nonvolatile processes. As shown in Figure 2, when we opened the X-ray beam shutter at time t = 39 s, the current level instantaneously increased by 4 orders of magnitude from 10^{-12} to 10^{-8} A. With the shutter closed at t = 50 s, the current level decreased rapidly to 10^{-10} A. At t = 77 s, we opened the shutter again. Then, the current level increased and the cell changed back to a lower resistance state, with a current level of about 10^{-8} A. This suggests that the resistance of the cell might be reversibly controlled by the X-ray irradiation (regime 1 of Figure 2). The resistance change observed when the cells are being irradiated by X-ray beams can be attributed to a volatile reversible process, since as soon

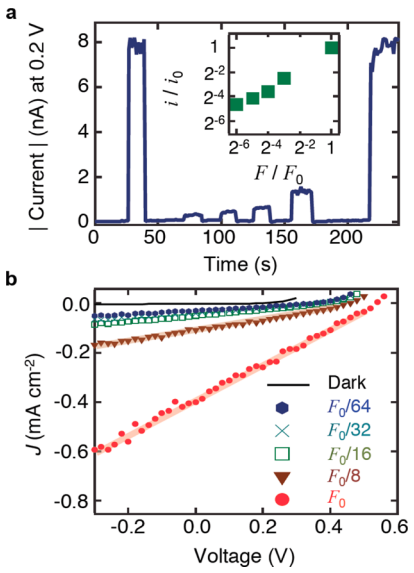

Figure 3. Photovoltaic-like effect induced by X-ray. (a) Reversible changes of current level at 0.2 V with the change of the intensity of X-ray beam. The inset shows the proportional relation between the relative current level (i/i_0) and the intensity of X-ray beam (F/F_0). (b) Current density–voltage (J–V) characteristics under the X-ray irradiation with different intensity of incident X-ray beam.

as the shutter is closed, the resistance starts to increase again.

However, there also occurs a nonvolatile process during the X-ray irradiation. For instance, the current level at t = 50 – 76 s (with the shutter closed after exposure of the X-ray beam) is 2 orders of magnitude higher than the pristine current level. Moreover, when t > 88 s, the current level started to gradually increase and change in a nonvolatile manner, as shown in the inset and regime 2 of Figure 2. Finally, the current level of the cell increased up to the compliance current level at approximately t = 2000 s (regime 3 of Figure 2). This drastic change of the current level is consistent with that of the previous result in Figure 1b. However, it should be noted that this change is different from the irreversible resistance change induced by only the uniform reduction of TiO_2 by, *e.g.*, Knotek–Feibelman mechanism[12] as we could change the state to HRS by applying electrical bias (see Supporting Information, Figure S1).

Photovoltaic-like Behavior. To achieve further insight into the origins of volatile reversible resistance changes induced by the X-ray irradiation, we varied the intensity (photon flux, F, and the incident total flux, F_0) of the X-ray beam incident on a Pt/TiO_2/Pt cell by controlling the number of aluminum (Al) attenuators in the setup for the X-ray experiments. As shown in Figure 3a, the current level of the cell at 0.2 V increased with the increase of the incident beam intensity. The inset of Figure 3a indicated that there exists a strong correlation between the resistance change and the incident beam intensity.

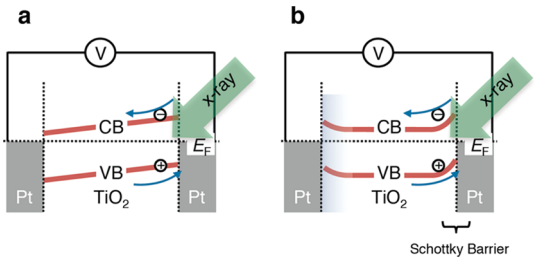

Figure 4. Schematic of photovoltaic-like effect. (a) The top Pt electrode and TiO_2 form Schottky barrier, of which width is larger than the film thickness leading to a fully depleted layer in TiO_2. (b) The top Pt electrode and TiO_2 form Schottky barrier, which is confined to the vicinity of electrode/interface region leading to a partial depletion in TiO_2. The former is related with lower defect density in the film, while the latter is related with higher defect density in the film.

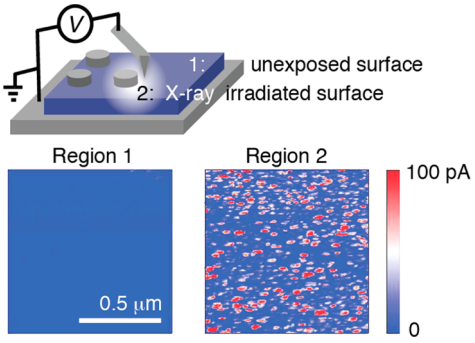

Figure 5. Schematic of C-AFM measurements and C-AFM images on Region 1 (the pristine surface) and Region 2 (the X-ray irradiated surface). Two-dimensional current map measured at 0.02 V in Regions 1 and 2 show distinct difference between unexposed pristine and X-ray irradiated regions. Conduction paths of 28 ± 14 nm diameter are clearly seen in Region 2.

As shown in Figure 3b, X-ray intensity-dependent current density–voltage (J–V) characteristics indicate that in the volatile reversible and spontaneous process there exists a photovoltaic-like effect. Asymmetric J–V curve of the dark current represents the existence of Schottky barrier at the interface between Pt electrodes and n-type TiO_2 (see Figure 4).[23,24] Note that the open-circuit voltage and short-circuit current density are 0.4–0.6 V and 0.03–0.4 mA/cm^2, respectively. They are dependent on the flux of the incident X-ray beam. External Quantum Efficiency (EQE) at the given energy is approximately 5×10^{-4}, where the incident photon flux is $F_0 = 2 \times 10^7/(\mu m^2\ s)$ (see Supporting Information).

C-AFM Measurement. We tested the local conductance of the cell using conducting atomic force microscope (C-AFM).[25] Figure 5 illustrates a schematic diagram of the C-AFM experimental setup and C-AFM images. We tested the bare surface of TiO_2 on the bottom Pt electrode using a solid Pt nanowire tip probe as the top electrode. As shown in Figure 5, two-dimensional current-maps measured at 20 mV to the tip indicated that the TiO_2 surface not covered with Pt top electrodes, which was irradiated for 24 h, changed into highly

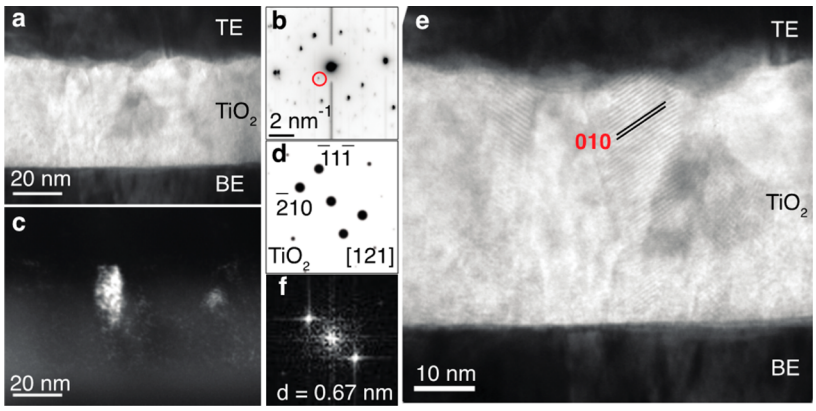

Figure 6. Cross-section TEM analysis of conducting filaments. (a) Bright field TEM image showing the TiO_2 film after irradiation between the top and bottom electrodes. (b) Selected area electron diffraction pattern from the region shown in (a). (c) Dark field TEM image showing the filament like region formed in the oxide film. (d) The diffraction pattern shows majority of the spots from the [121] zone axis of Brookite (simulated pattern). The spot highlighted in red with $d = 0.67$ nm was used to form the dark field image shown in (c). (e) The HREM image of the filament like region. (f) The diffractogram obtained from the same region. The lattice spacing of $d = 0.67$ nm is clearly seen which corresponds to [010] of the Magnéli phase of Ti_4O_7.

conducting state when compared to the state of the pristine surface. We found that there were 285 conducting channels (red regions) with average diameter of 28 ± 14 nm (see Supporting Information, Figure S2). On the other hand, we also found that the X-ray irradiated region covered with Pt top electrodes had far fewer conduction paths than the bare surface region exposed directly to X-rays. This supports the nonuniform and local nature of conducting filaments formed during the X-ray irradiation on the regions covered with Pt top electrodes (see Supporting Information, Figure S3). To confirm this, therefore, cross-section transmission electron microscopy (TEM) was performed.

TEM Observations. We used TEM to study the changes in the microstructure and correlate them with the observed change in the resistance of the $Pt/TiO_2/Pt$ cells. High-resolution TEM (HRTEM) images from the pristine sample show that the TiO_2 is polycrystalline and in the Brookite phase (see Supporting Information, Figure S4). Figure 6a shows a region from the X-ray irradiated sample underneath the top electrode and Figure 6b shows the selected area electron diffraction (SAED) pattern from this region. The dominant reflections in the SAED pattern can be identified as the Brookite $[\bar{2}10]$ and $[\bar{1}1\bar{1}]$ reflections from the simulated [121] zone axis pattern shown in Figure 6d. However, there are also other weaker reflections seen in the pattern corresponding to $d = 0.67$ nm (highlighted in red circle). This distance corresponds to the [010] lattice spacing of the Ti_4O_7 Magnéli phase, which shows metallic (Fermi liquid) behavior at $T > 130-150$ K (see Supporting Information, Figure S6).[20,26] The dark field TEM image formed using this spot is shown in Figure 6c, which highlights a filament-like region in the TiO_2 film.[20] HRTEM image of this region is shown in Figure 6e where the filament-like region with lattice fringes corresponding to $d = 0.67$ nm are clearly seen. Figure 6f shows the diffractogram from this region confirming the observed lattice spacing. This result conclusively shows the formation of Magnéli phase filaments within the TiO_2 film after irradiation. Also it should be noted that there were several such filaments observed within the TEM sample (see Supporting Information, Figure S5).

DISCUSSION

The resistance change induced by the X-ray irradiation occurs *via* two independent processes: reversible volatile photovoltaic-like process and nonvolatile formation of conduction paths that can be controlled reversibly by electric bias. As shown in Figure 4a, we believe that X-rays impinging on a sample generate core holes and Auger/hot (energetic) electrons, which can be transferred to the electrode by the internal electric field formed by fully depleted Schottky barriers (the depletion width $W \gg$ the film thickness d) at both electrode/oxide interfaces before the recombination.[27,28] Note that with the increase of the carrier concentrations ($>10^{18}$ cm^{-3}), the Schottky barrier can be confined to the vicinity of electrode/interface region ($W < d$),[28] as shown in Figure 4b. Therefore, the current can flow in the reverse direction with respect to the bias voltage and it can be tuned by an applied electric field and X-ray intensity. However, the nonvolatile reversible resistance change phenomenon (see the inset of Figure 2) cannot be fully explained by this photovoltaic-like effect.

To shed light on the mechanisms of the nonvolatile process (from regime 1 to regime 2 and from regime 2 to regime 3), two effects have to be discussed: X-ray induced defect generation and Joule-heating. These two effects are closely related to the formation of conducting paths (*i.e.*, Magnéli phase) in TiO_2-based resistance switching devices.[18] First, X-ray irradiation can create defects in transition metal oxides.[7,9,29] High-energy X-ray irradiation excites core electrons/holes

and successively induces Auger/hot (energetic) electrons.[27] The energetic electrons scatter with ions in the insulating oxides.[27] Then they break bonds and create defects, especially oxygen vacancies, which can form less-insulating phases. It is noted that the threshold fluence of the TiO_2 device (see the inset of Figure 2) is approximately 10^8–10^9 μm^{-2} (or 10^{16}–10^{17} cm^{-2}), which is comparable with that of other transition metal oxide systems.[9] Indeed, our C-AFM measurements demonstrated that the conductance map of the irradiated surface shows a more conducting state over the whole irradiated area when compared to the state of the pristine surface as shown in Figure 5.

Second, Joule-heating can contribute to the local formation of Magnéli phases in the Pt/TiO_2/Pt cells (especially from regime 2 to regime 3). Joule-heating increases the local temperature and enhances the drift and diffusion of oxygen[30] or electrochemical reduction in a solid electrolyte by, *e.g.*, the Fray–Farthing–Chen process.[26,31] In our case from regime 1 to regime 2 in Figure 3, X-rays initially induced current flow, which is lower than 0.3 mA/cm^2 at 0.2 V. If this current flows uniformly, the current level in regime 1 is too small to initiate a conventional external bias-driven forming process, which requires a current density[20] higher than 10^6 A/cm^2. However, if the current flow is confined to a path of a few tens of nanometers in diameter, the current density of regime 2, enhanced by the X-ray induced defect generation, will attain the necessary condition to undergo the local phase transition. We confirmed by TEM that the size of several conduction paths comprised of Magnéli phase was about 10–20 nm, which is also comparable to the average size of local conduction paths observed by C-AFM in Figure 5. Furthermore, our TEM results confirmed the formation of cone shaped Magnéli phase in TiO_2 films after irradiation, which has comparable size and shape (wider near cathode and narrower near anode) to that formed by voltage application with Joule heating effect.[20] We believe that the defects generated over the wider irradiated area (most probably oxygen vacancies) gathered together to form the Magnéli phase filaments during the long exposure time, which could be supplemented by the Joule-heating effect.

CONCLUSIONS

In summary, we found that X-ray induced conductance enhancement in Pt/TiO_2/Pt structures occurs *via* reversible volatile and nonvolatile processes. A reversible volatile change of the pristine resistance state indicates that a photovoltaic-like effect can modulate the conductance reversibly by a few orders of magnitude in response to the intensity of impinging X-rays. We also found that a reversible nonvolatile conductance change occurred when the photovoltaic-like effect is combined with a local phase transition into Magnéli phase, which was confirmed by TEM observation. Our discovery of a reversible resistance change induced by X-rays is unexpected, as the scattering cross-section of X-rays with TiO_2 is extremely small. However, our observations convincingly point toward the combined effects of a photovoltaic effect, Joule-heating and X-ray induced defect generation. The usual methods to control oxygen vacancies in resistive switching materials are known to require an external bias voltage or current. This X-ray irradiation effect can provide a novel methodology to initiate the electroforming process.

MATERIALS AND METHODS

Fabrication. We fabricated Pt/TiO_2/Pt cells by growing polycrystalline TiO_2 films on Pt/Si substrate using atomic layer deposition technique at a substrate temperature of 250 °C using $Ti(OC_3H_7)_4$ and O_3 as the Ti-precursor and oxygen source, respectively. The thickness of TiO_2 and diameter of electron-beam evaporated top electrode Pt were 40 nm and 50–300 μm, respectively.

Electrical Measurement. The current–voltage (I–V) curves of our Pt/TiO_2/Pt cells were measured by using a conventional two-probe measurement system (Keithley 237 Source Measure Unit). To avoid a complete dielectric breakdown, we used compliance current to set a limit to the current flow.

Synchrotron-Based X-ray Measurement. The X-ray irradiation measurements were acquired at sector 9ID-B of the Advanced Photon Source with an electrical probe tip. The incident X-ray energy was set at 8.3 keV and the incident photon flux was 2×10^7 photons/(μm^2 s). Beam size was 150 (V) μm $\times$ 600 (H) μm. During the X-ray irradiation, the TE was biased with 0.2 V to minimize the perturbations by, *e.g.*, Joule heating and oxygen vacancy drift in the system.[32] The color of the sample changed from blue to yellow after 24 h exposure to the X-ray beam.

Conducting Atomic Force Microscopy. Conducting AFM maps were obtained using the MFP-3D scanning probe microscope from Asylum Research with the ORCA sample mount and cantilever holder. Solid platinum C-AFM probes with tip radius <20 nm from Rocky Mountain Nanotechnology, LLC were used.

Transmission Electron Microscopy. TEM samples were prepared from using Focused Ion Beam (FIB, Zeiss 1540XB) lift out method from the pristine sample and the irradiated sample from underneath the top electrode area. Damage due to high energy (30 kV) Ga^+ ions was reduced by using low energy (0.5 kV) Ar^+ ion milling. High-resolution images and selected area electron diffraction patterns were acquired using the Tecnai F20 TEM operating at 200 kV. Damage due to incident electron beam was reduced by using lower beam current and exposure times. All the microscopy was performed at the Electron Microscopy Center at Argonne National Laboratory.

Conflict of Interest: The authors declare no competing financial interest.

Acknowledgment. The submitted manuscript has been created by UChicago Argonne, LLC, Operator of Argonne National Laboratory ("Argonne"). Argonne, a U.S. Department of Energy Office of Science laboratory, is operated under Contract No. DE-AC02-06CH11357. The U.S. Government retains for itself, and others acting on its behalf, a paid-up nonexclusive, irrevocable worldwide license in said article to reproduce, prepare derivative works, distribute copies to the public, and perform publicly and display publicly, by or on behalf of the

Government. Use of the Advanced Photon Source and Electron Microscopy Center of Argonne National Laboratory is gratefully acknowledged. C.S.H. acknowledges the support of Global Research Laboratory program (2012040157) through the National Research Foundation of Korea.

Supporting Information Available: Additional *I*−*V* curves, C-AFM and TEM figures, and EQE calculation. This material is available free of charge *via* the Internet at http://pubs.acs.org.

REFERENCES AND NOTES

1. Als-Noelsen, J.; McMorrow, D. *Elements of Modern X-ray Physics*; Wiley-CH: Weinheim, 2001.
2. Hau-Riege, S. P. *High-Intensity X-rays-Interaction with Matter: Processes in Plasmas, Clusters, Molecules and Solids*; Wiley-CH: Weinheim, 2012.
3. Fong, D. D.; Stephenson, G. B.; Streiffer, S. K.; Eastman, J. A.; Auciello, O.; Fuoss, P. H.; Thompson, C. Ferroelectricity in Ultrathin Perovskite Films. *Science* **2004**, *304*, 1650–1653.
4. Kim, J.; Casa, D.; Upton, M. H.; Gog, T.; Kim, Y.-J.; Mitchell, J. F.; Veenendaal, M.; van Daghofer, M.; Brink, J.; van den Khaliullin, G.; *et al.* Magnetic Excitation Spectra of Sr_2IrO_4 Probed by Resonant Inelastic X-Ray Scattering: Establishing Links to Cuprate Superconductors. *Phys. Rev. Lett.* **2012**, *108*, 177003–177007.
5. Janousch, M.; Meijer, G. I.; Staub, U.; Delley, B.; Karg, S. F.; Andreasson, B. P. Role of Oxygen Vacancies in Cr-Doped $SrTiO_3$ for Resistance-Change Memory. *Adv. Mater.* **2007**, *19*, 2232–2235.
6. Münstermann, R.; Yang, J. J.; Strachan, J. P.; Medeiros-Ribeiro, G.; Dittmann, R.; Waser, R. Morphological and Electrical Changes in TiO_2 Memristive Devices Induced by Electroforming and Switching. *Phys. Status Solidi RRL* **2010**, *4*, 16–18.
7. Kiryukhin, V.; Casa, D.; Hill, J. P.; Keimer, B.; Vigliante, A.; Tomioka, Y.; Tokura, Y. An X-ray-Induced Insulator-Metal Transition in a Magnetoresistive Manganite. *Nature* **1997**, *386*, 813–815.
8. Polli, D.; Rini, M.; Wall, S.; Schoenlein, R. W.; Tomioka, Y.; Tokura, Y.; Cerullo, G.; Cavalleri, A. Coherent Orbital Waves in the Photo-Induced Insulator−Metal Dynamics of a Magnetoresistive Manganite. *Nat. Mater.* **2007**, *6*, 643–647.
9. Poccia, N.; Fratini, M.; Ricci, A.; Campi, G.; Barba, L.; Vittorini-Orgeas, A.; Bianconi, G.; Aeppli, G.; Bianconi, A. Evolution and Control of Oxygen Order in a Cuprate Superconductor. *Nat. Mater.* **2011**, *10*, 733–736.
10. Analytis, J. G.; Ardavan, A.; Blundell, S. J.; Owen, R. L.; Garman, E. F.; Jeynes, C.; Powell, B. J. Effect of Irradiation-Induced Disorder on the Conductivity and Critical Temperature of the Organic Superconductor κ-(BEDT-TTF)$_2$Cu(SCN)$_2$. *Phys. Rev. Lett.* **2006**, *96*, 177002–177005.
11. Kurtz, R. L.; Stockbauer, R.; Madey, T. E. Angular Distributions of Ions Desorbing from TiO_2. *Nucl. Instrum. Methods Phys. Res.* **1986**, *B 13*, 518–524.
12. Knotek, M. L.; Feibelman, P. J. Stability of Ionically Bonded Surfaces in Ionizing Environments. *Surf. Sci.* **1979**, *90*, 78–90.
13. Waser, R.; Aono, M. Nanoionics-Based Resistive Switching Memories. *Nat. Mater.* **2007**, *6*, 833–840.
14. Strukov, D. B.; Snider, G. S.; Stewart, D. R.; Williams, R. S. The Missing Memristor Found. *Nature* **2008**, *453*, 80–83.
15. Terabe, K.; Hasegawa, T.; Nakayama, T.; Aono, M. Quantized Conductance Atomic Switch. *Nature* **2005**, *433*, 47–50.
16. Ohno, T.; Hasegawa, T.; Tsuruoka, T.; Terabe, K.; Gimzewski, J. K.; Aono, M. Short-Term Plasticity and Long-Term Potentiation Mimicked in Single Inorganic Synapses. *Nat. Mater.* **2011**, *10*, 591–595.
17. Dearnaley, G.; Stoneham, A. M.; Morgan, D. V. Electrical Phenomena in Amorphous Oxide Films. *Rep. Prog. Phys.* **1970**, *33*, 1129–1191.
18. Choi, B. J.; Jeong, D. S.; Kim, S. K.; Rohde, C.; Choi, S.; Oh, J. H.; Kim, H. J.; Hwang, C. S.; Szot, K.; Waser, R.; *et al.* Resistive Switching Mechanism of TiO_2 Thin Films Grown by Atomic-Layer Deposition. *J. Appl. Phys.* **2005**, *98*, 033715.
19. Kim, K. M.; Jeong, D. S.; Hwang, C. S. Nanofilamentary Resistive Switching in Binary Oxide System; a Review on the Present Status and Outlook. *Nanotechnology* **2011**, *22*, 254002–2540018.
20. Kwon, D.-H.; Kim, K. M.; Jang, J. H.; Jeon, J. M.; Lee, M. H.; Kim, G. H.; Li, X.-S.; Park, G.-S.; Lee, B.; Han, S.; *et al.* Atomic Structure of Conducting Nano-Filaments in TiO_2 Resistive Switching Memory. *Nat. Nanotechnol.* **2010**, *5*, 148–153.
21. Chang, S. H.; Lee, J. S.; Chae, S. C.; Lee, S. B.; Liu, C.; Kahng, B.; Kim, D.-W.; Noh, T. W. Occurrence of Both Unipolar Memory and Threshold Resistance Switching in a NiO Film. *Phys. Rev. Lett.* **2009**, *102*, 026801–026804.
22. Chae, S. C.; Lee, J. S.; Kim, S.; Lee, S. B.; Chang, S. H.; Liu, C.; Kahng, B.; Shin, H.; Kim, D.-W.; Jung, C. U.; *et al.* Random Circuit Breaker Network Model for Unipolar Resistance Switching. *Adv. Mater.* **2008**, *20*, 1154–1159.
23. Yang, J. J.; Picket, M. D.; Li, X.; Ohlberg, D. A. A.; Stewart, D. R.; Williams, R. S. Memristive Switching Mechanism for Metal/Oxide/Metal Nanodevices. *Nat. Nanotechnol.* **2008**, *3*, 429–433.
24. Kim, H.; Hong, S.; Kim, D.-W. Ambient Effects on Electric-Field-Induced Local Charge Modification of TiO_2. *Appl. Phys. Lett.* **2012**, *100*, 022901.
25. Chang, S. H.; Lee, S. B.; Jeon, D. Y.; Park, S. J.; Kim, G. T.; Yang, S. M.; Chae, S. C.; Yoo, H. K.; Kang, B. S.; Lee, M.-J.; *et al.* Oxide Double Layer Nanocrossbar for Ultrahigh-Density Bipolar Resistance Switching Memory. *Adv. Mater.* **2011**, *23*, 4063–4067.
26. Szot, K.; Rogala, M.; Speier, W.; Klusek, Z.; Besmehn, A.; Waser, R. TiO_2—a Prototypical Memristive Material. *Nanotechnology* **2011**, *22*, 254001–254021.
27. Cazaux, J. A Physical Approach to the Radiation Damage Mechanisms Induced by X-rays in X-ray Microscopy and Related Techniques. *J. Microsc.* **1997**, *188*, 106–124.
28. Kim, K. M.; Choi, B. J.; Shin, Y. C.; Choi, S.; Hwang, C. S. Anode-Interface Localized Filamentary Mechanism in Resistive Switching of TiO_2 Thin Films. *Appl. Phys. Lett.* **2007**, *91*, 012907.
29. Garganourakis, M.; Scagnoli, V.; Huang, S. W.; Staub, U.; Wadati, H.; Nakamura, M.; Guzenko, V. A.; Kawasaki, M.; Tokura, Y. Imprinting Magnetic Information in Manganite's with X-rays. *Phys. Rev. Lett.* **2012**, *109*, 157203–157207.
30. Yang, J. J; Strukov, D. B.; Stewart, D. R. Memristive Devices for Computing. *Nat. Nanotechnol.* **2013**, *8*, 13–24.
31. Chen, G. Z.; Fray, D. J.; Farthing, T. W. Direct Electrochemical Reduction of Titanium Dioxide to Titanium in Molten Calcium Chloride. *Nature* **2000**, *407*, 361–364.
32. Yang, J. J.; Miao, F.; Pickett, M. D.; Ohlberg, D. A. A.; Stewart, D. R.; Lau, C. N.; Williams, R. S. The Mechanism of Electroforming of Metal Oxide Memristive Switches. *Nanotechnology* **2009**, *20*, 215201.